Results in Engineering 25 (2025) 104588

Contents lists available at ScienceDirect

Results in Engineering

journal homepage: www.sciencedirect.com/journal/results-in-engineering

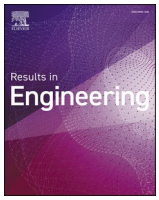

Research paper

Ultrasonic welding of ground tire rubber-filled polypropylene blends

Ákos Görbe [a,b], Péter Széplaki [a,b], Tamás Bárány [a,b,c,*]

[a] Department of Polymer Engineering, Faculty of Mechanical Engineering, Budapest University of Technology and Economics, Műegyetem rkp. 3., H-1111 Budapest, Hungary
[b] PolymerOn Ltd., Háros u. 7., H-1222 Budapest, Hungary
[c] MTA-BME Lendület Lightweight Polymer Composites Research Group, Műegyetem rkp. 3., H-1111 Budapest, Hungary

ARTICLE INFO

Keywords:
Ground tire rubber
Devulcanization
Dynamic vulcanization
Thermoplastic elastomers
Ultrasonic welding
Circular economy
Rubber recycling

ABSTRACT

In this study, we examined the weldability of thermoplastic elastomers made from ground tire rubber (GTR) with polypropylene and explored the effects of devulcanized GTR (dGTR) and dynamic vulcanization to produce thermoplastic dynamic vulcanizates (TDV). We characterized the damping properties of blends and revulcanized dGTR and found that increasing load does not affect the damping of the rubber, but the blends behaved similarly to polypropylene. We examined the effect of welding force and time on welds between polypropylene and the blends and found that both time and force have an optimum for the best maximum force and elongation: the best properties were examined with 0.3 s of weld time and 200 N of weld force. Similar trends were observed in welds between identical blend types. We also examined the morphology of the seams and found that both devulcanization and dynamic vulcanization helped to distribute the rubber phase better, which resulted in seams with smaller rubber particles that can act as defects. With Taguchi analysis we determined that the best weld quality was achieved between TDV and PP at 300 N of weld force. We also showed that no specimen exhibited voids and cracks in the seam. Our findings show that filling GTR or dGTR in polypropylene results in a rubber-like thermoplastic material which is also characterized by good weldability. This article shows an application of inserting GTR into circular economy.

1. Introduction

Recycling is one of the most important issues the polymer industry faces. While numerous studies have dealt with the recyclability of thermoplastic polymers, particularly focusing on bottles due to their majority in plastic waste [1], recycling rubber waste presents its challenge [2–4]. Unlike thermoplastics, rubbers present a greater challenge in recycling: their elasticity stems from crosslinks within their molecular chains. However, these crosslinks block reversible melting, making their recycling process more complex [5]. The most pressing issue with rubber waste is waste tires: the amount of them is expected to reach 3.4 billion tons annually in 2050 [6]. After dismantling, the tire rubber can be shredded thus ground tire rubber (GTR) is formulated [7]. GTR can be used in a wide range of applications, from mixing into asphalt to covering artificial grass and other types of surfaces [7,8]. The most viable usage is to take it back to the source and use it as building blocks of new rubber goods or fill thermoplastic materials with it. Filling thermoplastic materials with GTR is not a new practice; it is used to improve the toughness of these plastics [9,10]. However, compatibility between the GTR and the thermoplastic is poor, which means that in order to achieve high performance, some kind of compatibilization is necessary [11,12].

One possible way to compatibilize the phases is also used in the recycling of rubber waste: devulcanization and reclamation aim to break up crosslinks between the molecules [13]. This makes the rubber reformable and usable in virgin rubber compounds and enhances compatibility with the thermoplastic matrix by mobilizing the molecules in rubber. Devulcanization accomplishes the objective through selective crosslink scission, while reclamation involves chain scission [14]. This means that devulcanization is the more sought-after concept since selective crosslink scission does not worsen the material's properties as much as chain scission. Various methods exist for devulcanization, with the most prevalent being thermomechanical [15–18], thermochemical [19], and microwave devulcanization [20–22].

Devulcanized ground tire rubber (dGTR) can be blended with thermoplastic materials to produce thermoplastic elastomers (TPE). TPEs exhibit rubber-like behavior due to their physical crosslinked structure while being reversibly meltable, granting easy recyclability [23]. One

* Corresponding author.
E-mail address: barany.tamas@gpk.bme.hu (T. Bárány).

https://doi.org/10.1016/j.rineng.2025.104588
Received 8 December 2024; Received in revised form 10 February 2025; Accepted 5 March 2025
Available online 6 March 2025

special group of TPEs is polymer-elastomer blends, which gain their rubbery behavior thanks to finely dispersed rubber domains in a thermoplastic matrix [24,25]. The particle size of the rubber phase is essential to be in the micrometer range for rubber-like behavior, which can be achieved via dynamic vulcanization [26–28]. In this process, the rubber mixture is fed into the processing equipment in its unvulcanized form; vulcanization occurs in situ during the compounding under intensive shearing [29,30]. It reduces the size of the rubber domains, resulting in thermoplastic dynamic vulcanizate (TDV).

TDVs are commercially available materials (e.g., Santoprene®) that are composed of polypropylene (PP) and ethylene propylene diene monomer rubber (EPDM). They are characterized by high elongation and good recyclability, but they are more expensive compared to conventional rubbers, so manufacturers are reluctant to change [31]. Using GTR to produce TPEs would not only lower the price but also be an innovative way to insert rubber waste into the circular economy [32].

Using a rubber coating would have several advantages for many products, as it would greatly increase the resistance to external forces and make the product much tougher [33]. The problem is, however, that for classic cross-linked rubbers, this coating is very costly and complicated due to vulcanization processes (e.g., the need for a special formulation, additional equipment and professional knowledge that an injection molding company does not always have). The solution to this issue could be the application of welding, which is also a common process of joining in the industry [34].

Ultrasonic welding is one of the most popular and commonly used welding processes. It is a very clean and versatile technology that uses mechanical vibrations to generate interfacial heating and melting to weld the components together [35]. For the rubber, melting is a crucial problem, but using TPE could eliminate this. A thermoplastic part of a TPE blend can be an excellent way to create welded joints. In this case, the GTR would act as a filler, changing the product's mechanical properties.

The effect of fillers on ultrasonic weldability is an area that has been heavily researched. However, the primary focus here is not on elastic fillers like GTR, but rather on traditional fiber reinforcements, which enhance stiffness and tensile strength. The well known factors that influence the weld quality are welding power, welding time, welding force, the use of energy director, or the presence of moisture [36,37]. However, because of the obvious differences between a reinforcing fiber and a GTR, whether mechanical or morphological, the previously shown guidelines cannot be taken as fundamental as the damping of the GTR can cause difficulties in ultrasonic welding. Consequently, the effect of these parameters on the weld quality as a function of the filler material has to be investigated. The weldability of TPEs is an area that has hardly been explored but offers great potential because it could be worthwhile from a manufacturing and economic point of view. Moreover, no study has dealt with the weldability of GTR-filled thermoplastic materials. In this study, we investigated the weldability of PP-based TPEs with recycled rubber using ultrasonic welding for sustainable applications.

2. Materials and methods

2.1. Materials

We used R660 polypropylene random copolymer (extrusion grade, MFI (2.16 kg, 230 °C) 2 g/10 min) provided by MOL Petrochemicals Ltd (Tiszaújváros, Hungary). We used this PP for compounding and welding experiments.

Devulcanized ground tire rubber (dGTR) was provided by Tyromer Inc. (Waterloo, ON, Canada). Ground tire rubber, made from truck tires with a particle size under 1 mm, is thermomechanically devulcanized in an extruder with the help of supercritical CO_2. The company also provided the original GTR they used during the process.

We used the curatives and additives presented in the rubber phase of the TDVs (Table 1).

Table 1
Materials used for curing the rubber phase of the TDV.

Material	Manufacturer	Trademark	Function
ZnO	Werco Metal (Zlatna, Romania)	–	Activator
Stearic acid	Oleon (Ertvelde, Belgium)	Radiacid 0154	
CBS N-cyclohexyl-2-benzothiazolesulfenamide	Rhein Chemie (Mannheim, Germany	Rhenogran CBS-80	Accelerator
Sulfur	Ningbo Actmix Polymer (Ningbo, Zhejiang, China)	ACTMIX S-80	Curing agent

Table 2
Recipe for the rubber phase.

	Amount of ingredient (phr)
dGTR	100
ZnO	5
stearic acid	2
CBS	1.5
Sulfur	1.5

Table 3
Formulation of the compounds.

Compound	Components
PP_GTR	40 wt% PP + 60 wt% GTR
PP_dGTR	40 wt% PP + 60 wt% dGTR
PP_TDV	40 wt% PP + 60 wt% dGTR dynamically vulcanized

Table 4
Samples for the preliminary tests.

Sample name	Component 1	Component 2	Welding force (N)	Welding time (s)
trial1	PP_TDV	PP_R660	300	0.1
trial2	PP_TDV	PP_R660	300	0.2
trial3	PP_TDV	PP_R660	300	0.3
trial4	PP_TDV	PP_R660	300	0.5

2.2. Preparation of TDVs

We prepared the rubber phase of the TDVs using a Brabender Lab-Station internal mixer (Brabender GmbH & Co. KG (Duisburg, Germany)) equipped with a W 350 E chamber (free volume 370 cm^3). The temperature was set to 50 °C, and the batches were mixed at 40 rpm. The recipe is presented in Table 2.

We prepared the compounds with a twin-screw extruder (Labtech Engineering Co., Ltd., Samutprakarn, Thailand) with a revolution speed of 120 rpm. The compositions of the compounds are listed in Table 3.

We prepared flat specimens of both the TDVs and the reference PP by injection molding using an Arburg Allrounder Advance 270S 400–170 type (Arburg GmbH, Lossburg, Germany) injection molding machine with a temperature profile of 190/190/185/180/175/45 °C.

2.3. Ultrasonic welding

We used a Herrmann Ultraschalltechnik HiQ Evolution Speed Control (Herrmann Ultraschalltechnik, Brunn am Gebirge, Austria) ultrasonic welder for the welding experiments. We created the welds on 20 mm wide flat specimens with a frequency of 20 kHz and an overlapping of 15 mm x 20 mm. To determine the adequate parameters, we performed preliminary tests with parameters shown in Table 4.

Table 5
Samples for the welding tests.

Sample name	Component 1	Component 2	Welding force (N)
PP_GTR150	PP_GTR	PP_R660	150
PP_GTR200	PP_GTR	PP_R660	200
PP_GTR300	PP_GTR	PP_R660	300
PP_dGTR150	PP_dGTR	PP_R660	150
PP_dGTR200	PP_dGTR	PP_R660	200
PP_dGTR300	PP_dGTR	PP_R660	300
PP_TDV150	PP_TDV	PP_R660	150
PP_TDV200	PP_TDV	PP_R660	200
PP_TDV300	PP_TDV	PP_R660	300
GTR150	PP_GTR	PP_GTR	150
GTR200	PP_GTR	PP_GTR	200
GTR300	PP_GTR	PP_GTR	300
dGTR150	PP_dGTR	PP_dGTR	150
dGTR200	PP_dGTR	PP_dGTR	200
dGTR300	PP_dGTR	PP_dGTR	300
TDV150	PP_TDV	PP_TDV	150
TDV200	PP_TDV	PP_TDV	200
TDV300	PP_TDV	PP_TDV	300

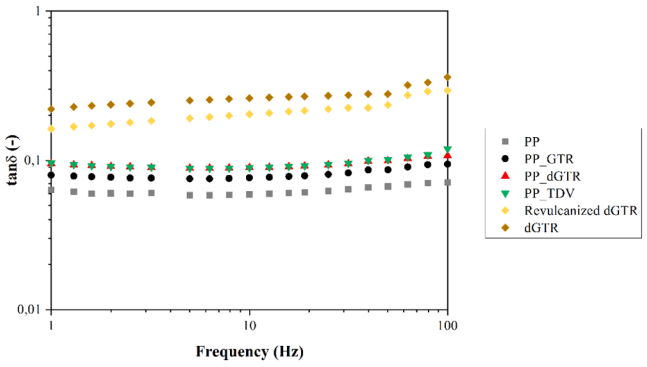

Fig. 1. Results of the DMTA tests.

We performed welds with parameters listed in Table 5 (welding time was fixed at 0.3 s).

2.4. Characterization methods

We performed dynamic mechanical thermical analysis (DMTA) tests using a TA Instruments Q800 (TA Instruments, United States) DMA tester in tensile mode to evaluate the damping properties of the materials. A frequency sweep was performed on the specimens at 30 °C between 1 and 100 Hz (at least 5 measurements at each level). The amplitude was chosen previously according to an amplitude sweep at 10 Hz at 30 °C. We determined the border of linear viscoelasticity based on 30 measuring points at every amplitude and chose an adequate amplitude for the frequency sweep.

We characterized the effect of ultrasonic loads on revulcanized rubber using Horikx's analysis [15] on 5 replicates. Horikx's analysis is a method that establishes a relationship between the soluble content and the decrease in crosslink density after devulcanization. The soluble fraction of the dGTR samples was determined by Soxhlet extraction in toluene, and the decrease in crosslink density was determined with swelling.

The crosslink density of the samples was determined using the equilibrium swelling test method. The samples were soaked in toluene for 72 h at room temperature as recommended by ASTM D6814–02 (2018). After that, the samples were removed from the solvent, dried with paper towels, and the swollen mass was measured. The samples were then dried at 80 °C for 12 h and their mass was measured again.

We calculated the crosslink density using the Flory–Rehner equation (Eq. (1)).

$$\nu_e = \frac{-[\ln(1-V_r) + V_r + \chi \cdot V_r^2]}{\left[V_s \cdot \left(V_r^{\frac{1}{3}} - \frac{V_r}{2}\right)\right]} \quad (1)$$

where ν_e is crosslink density (mol/cm^3), V_s is the molar volume of the solvent (for toluene: 106.27 cm^3/mol), χ is the Flory–Huggins interaction parameter (0.391), and V_r is the volume fraction of rubber in the swollen network. V_r can be calculated using the Ellis–Welding equation (Eq. (2)).

$$V_r = \frac{\frac{m_r}{\rho_r}}{\frac{m_r}{\rho_r} + \frac{m_s}{\rho_s}} \quad (2)$$

where m_r is the weight of the dry sample (g), m_s is the weight of the solvent absorbed by the sample (g), ρ_r is the density of the rubber sample (g/cm^3), and ρ_s is the density of the solvent (for toluene: 0.867 g/cm^3).

We also determined the swelling index (%) of the samples using Eq. (3).

$$Swelling\ index = \frac{m_{sr} - m_r}{m_r} \quad (3)$$

where m_{sr} is the weight of the swollen sample (g).

The density of the samples was determined according to the ASTM D 297–93 standard (hydrostatic method) with a Sartorius Quintix 125D semi-micro balance with a resolution of 0.01 mg. The test medium was distilled water with a temperature of 20.8 °C and a corresponding density of 0.998 g/cm^3.

We determined the soluble content of the treated samples with Soxhlet extraction. We performed the examination in boiling toluene for 24 h and determined the soluble content with Eq. (4).

$$Sol\ fraction = \left(1 - \frac{m_f}{m_i}\right) \cdot 100 \quad (4)$$

where m_f and m_i stand for the mass of rubber before and after extraction, respectively.

We performed shear tests on the welded specimens to measure their weld strength on 5 specimens. A Zwick Z005 (Zwick GmbH (Ulm, Germany)) universal testing machine with 5 kN load cell was used with a 100 mm/min crosshead speed.

We used a Keyence VHX-5000 (Keyence Corporation (Mechelen, Belgium)) light microscope. We examined the cross-section of the welded specimens to find defects in the weld, and we also defined the ratio of the overlapping and the actual welded area. We titled this index weld efficiency, and it can be calculated according to Eq. (5):

$$WE = \frac{L_r}{L_t} \cdot 100 \quad (5)$$

where WE is weld efficiency (%), L_r is the real length of the weld (mm), and L_t is the theoretical length of the weld (mm).

We performed all microscopical examinations on welded specimens embedded in epoxy resin. We ground and polished these samples using a Struers LaboPol-5 (Struers A/S, Netherlands) in 7 steps according to manufacturer advice.

Optimal welding conditions can be determined with Taguchi analysis [38]. We defined the maximum force as the most important factor, as it signals the load bearing of the seam. We determined two factors: type of blend and welding force, then calculated the signal to noise ratio according to Eq. (6):

$$\frac{S}{N} = -10 \cdot \log_{10}\left(\frac{1}{n} \cdot \sum_{i=1}^{n} \frac{1}{y_i^2}\right) \quad (6)$$

where S/N is the signal/noise ratio (-), n is number of measurements (-)

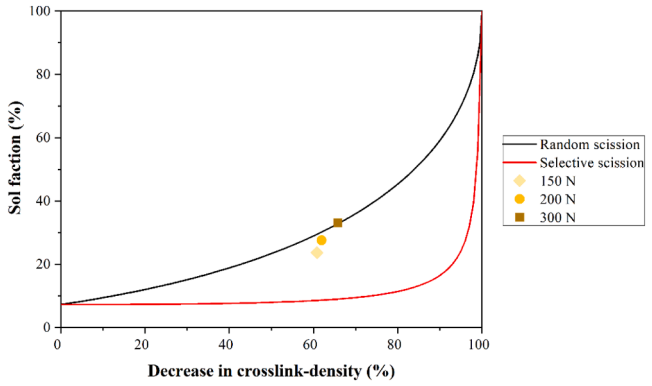

Fig. 2. Horikx's analysis of the revulcanized rubbers subjected to ultrasonic treatment.

Table 6
The results of the Horikx's analysis.

Welding force (N)	Sol fraction (%)	Decrease in crosslink-density (%)
150	23.6 ± 6.5	60.8
200	27.5 ± 4.6	61.8
300	33.1 ± 1.6	65.8

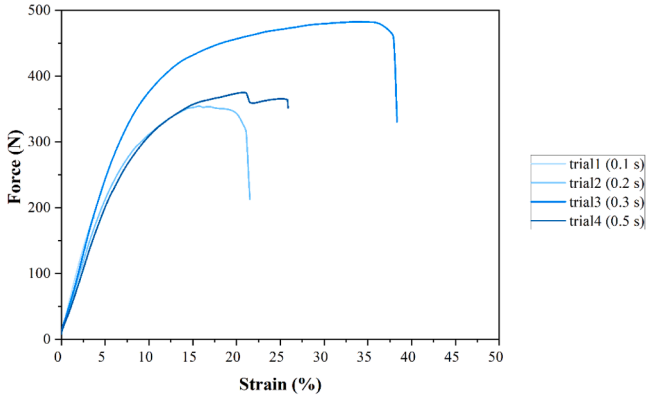

Fig. 3. Typical force-strain curves of the preliminary welds.

Table 7
Maximum force and strain for the trials.

	Maximum force (N)	Maximum strain (%)
trial1 (0.1 s)	233.4 ± 40.6	6.3 ± 2.7
trial2 (0.2 s)	378.1 ± 38.7	36.2 ± 15.3
trial3 (0.3 s)	452.7 ± 30.1	53.9 ± 12.8
trial4 (0.5 s)	380.2 ± 41.3	26.5 ± 5.2

y_i is the observed value. The S/N values were compared to each other, and since we want to maximize the load bearing capacity of the seam, the maximal value of S/N means the best parameter. We also created an interaction plot to visualize the results.

3. Results and discussion

We performed DMTA tests (Fig. 1) to investigate the damping (tanδ) of the blends, as it is a key factor in creating good welds with ultrasonic welding. We found that the damping of the blends lies between the damping of the PP and the revulcanized dGTR. Even though all blends contain only 40 wt% of PP, their damping is closer to PP than the neat and revulcanized dGTR. This can be caused by the morphology of the

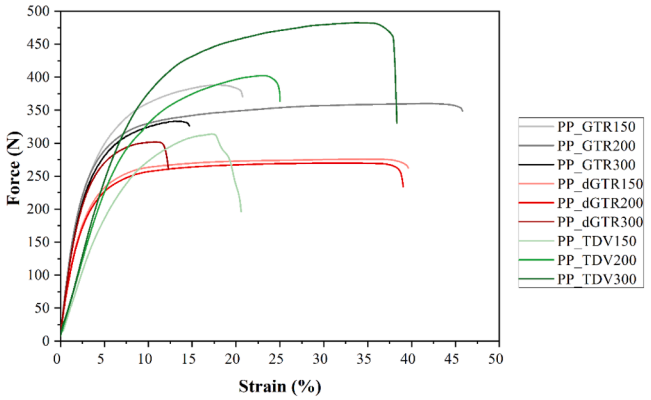

Fig. 4. Typical force-strain curves of the welds between the blends and polypropylene.

Table 8
Maximum force, strain and weld efficiency of the welds between the blends and polypropylene.

	Maximum force (N)	Maximum strain (%)	Weld efficiency (%)
PP_GTR150	431.3 ± 50.8*	31.4 ± 11.7	68
PP_GTR200	341.4 ± 41.2	45.3 ± 17.4	55
PP_GTR300	324.5 ± 44.5	18.9 ± 8.4	52
PP_dGTR150	274.6 ± 45.7*	37.8 ± 12.5	79
PP_dGTR200	269.6 ± 21.9	40.8 ± 19.4	68
PP_dGTR300	251.1 ± 41.4	16.7 ± 7.2	62
PP_TDV150	343.1 ± 51.4	14.6 ± 4.4	83
PP_TDV200	392.9 ± 62.7	26.3 ± 6.5	71
PP_TDV300	452.7 ± 30.1	53.9 ± 12.8	67

* the break initiated at the seam.

blends: they are characterized by finely dispersed fillers in the PP matrix, and the damping properties of the matrix are more dominant in this case. There is no significant change in the damping of the blends, which suggests that there is no difference in the weldability between the blends. It is also evident that the damping can be reduced with devulcanization, which can also help with creating better seams. It is also evident that increasing frequency does not influence the daming of the blends. However, increasing the frequency results in a slight increase of damping in the case of rubber and devulcanized rubber which can imply molecular degradation.

3.1. Horikx's analysis

Horikx's analysis (Fig. 2, Table 6) shows the effect of increasing welding force on the molecular structure of the revulcanized rubber. The results align more closely with the random scission curve, indicating that scission under these conditions is random rather than selective. As the force increases, the sol fraction grows, along with a greater reduction in crosslink density. This indicates that ultrasonic loads applied during the welding process led to the cleavage of both crosslinks and polymer backbones. Additionally, increasing the welding force amplifies this effect by promoting greater scission of the polymer chains.

3.2. Welding trials

In the case of the welding trials (Fig. 3, Table 7), it can be seen that increasing welding time increases both the maximum strength and the maximum elongation. If we increase welding time, molecular chains will be allowed more time to intertwine and form good-quality connections. However, there seems to be an optimum for welding times: after 0.3 s, a clear decline can be seen in the results. A degradation of the material can cause this. If the welding times are increased, the intensive stress (and

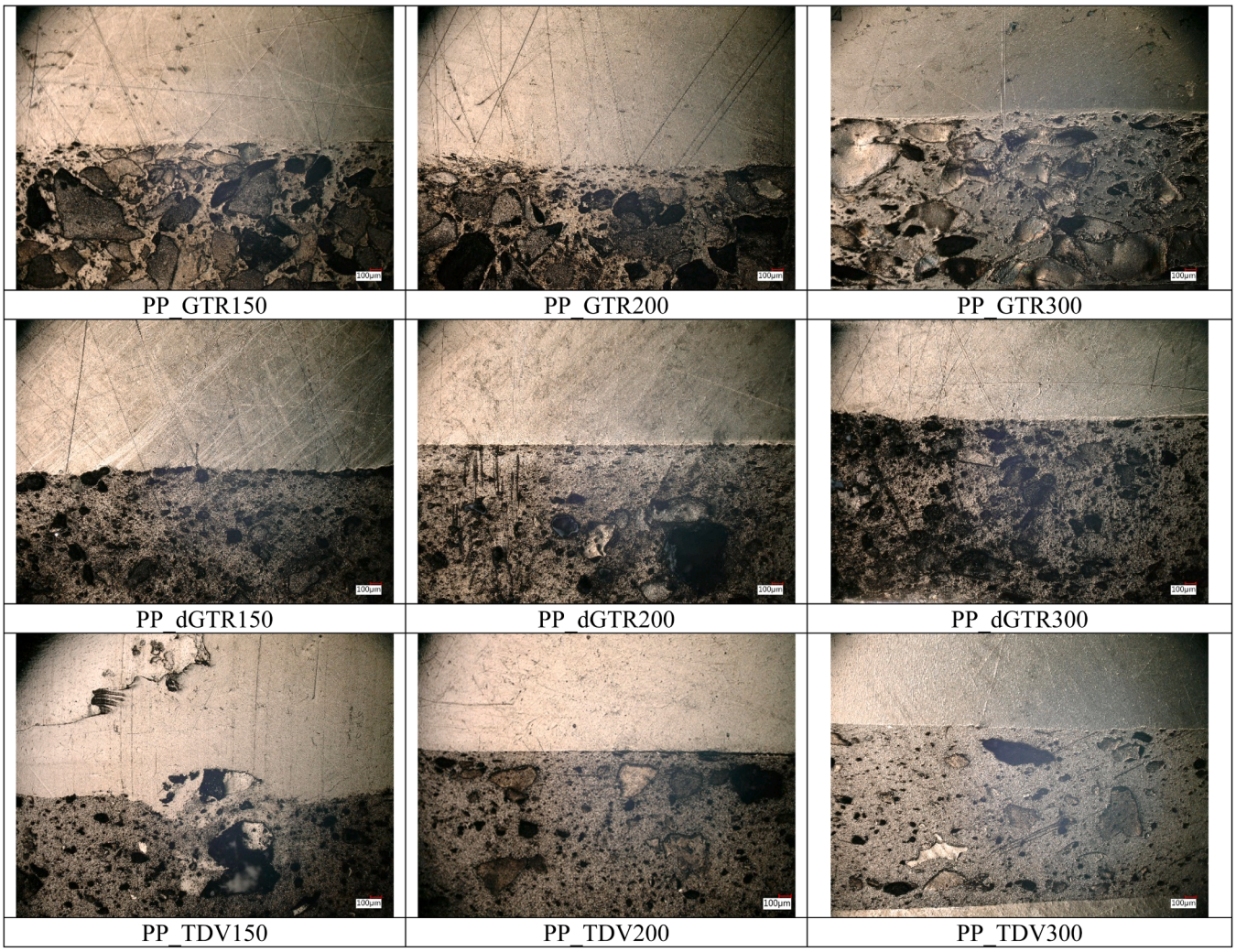

Fig. 5. Morphology of the welds between the blends and polypropylene.

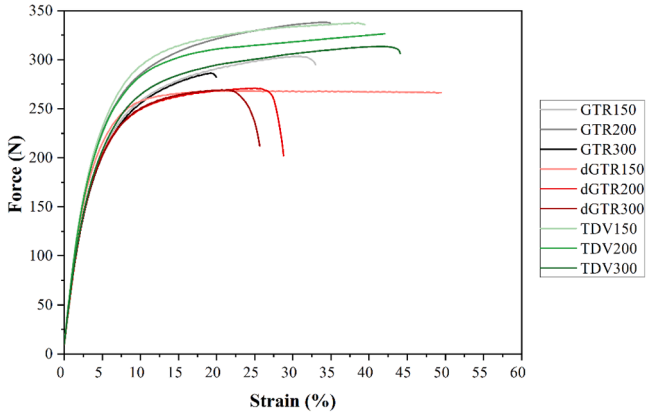

Fig. 6. Typical force-strain curves of the welds between the blends.

resulting heat) can cause both the molecular chains and the interface between phases to deteriorate. Therefore, the 0.3 s welding time provides sufficient time for the molecular chains to connect, but it degrades the materials much less than longer times.

Table 9
Maximum force, extension and weld efficiency of the welds between the blends.

	Maximum force (N)	Maximum extension (%)	Weld efficiency (%)
GTR150	307.1 ± 10.7	43.6 ± 15.7	71
GTR200	319.7 ± 22.4	32.5 ± 14.6	65
GTR300	296.6 ± 19.6	25.2 ± 7.2	60
dGTR150	274.2 ± 32.9	52.8 ± 20.2	81
dGTR200	286.9 ± 35.2	30.1 ± 12.3	74
dGTR300	249.8 ± 32.1	25.9 ± 10.5	70
TDV150	314.7 ± 26.5	39.7 ± 15.4	85
TDV200	293.8 ± 24.1	42.7 ± 5.8	80
TDV300	282.6 ± 43.2	43.1 ± 7.3	78

3.3. *Welding of PP and blends*

We studied the effect of welding forces on the welding efficiency, maximal force, and strain of the welded PP and GTR-PP blends (Fig. 4, Table 8). We found that both maximum force and strain have an inflexion point at 200 N in the case of GTR-filling. This can be caused by a similar effect as the one we have seen with welding times: if the force is too small, the molecule chains are not close enough to make sufficient contact; but if it is too large, the chains would degrade due to the increased heat generated by friction. In addition, Horikx's analysis (Fig. 2) revealed that the ultrasonic loads used for welding also causes cleavage of both crosslinks and the backbone. During the welding

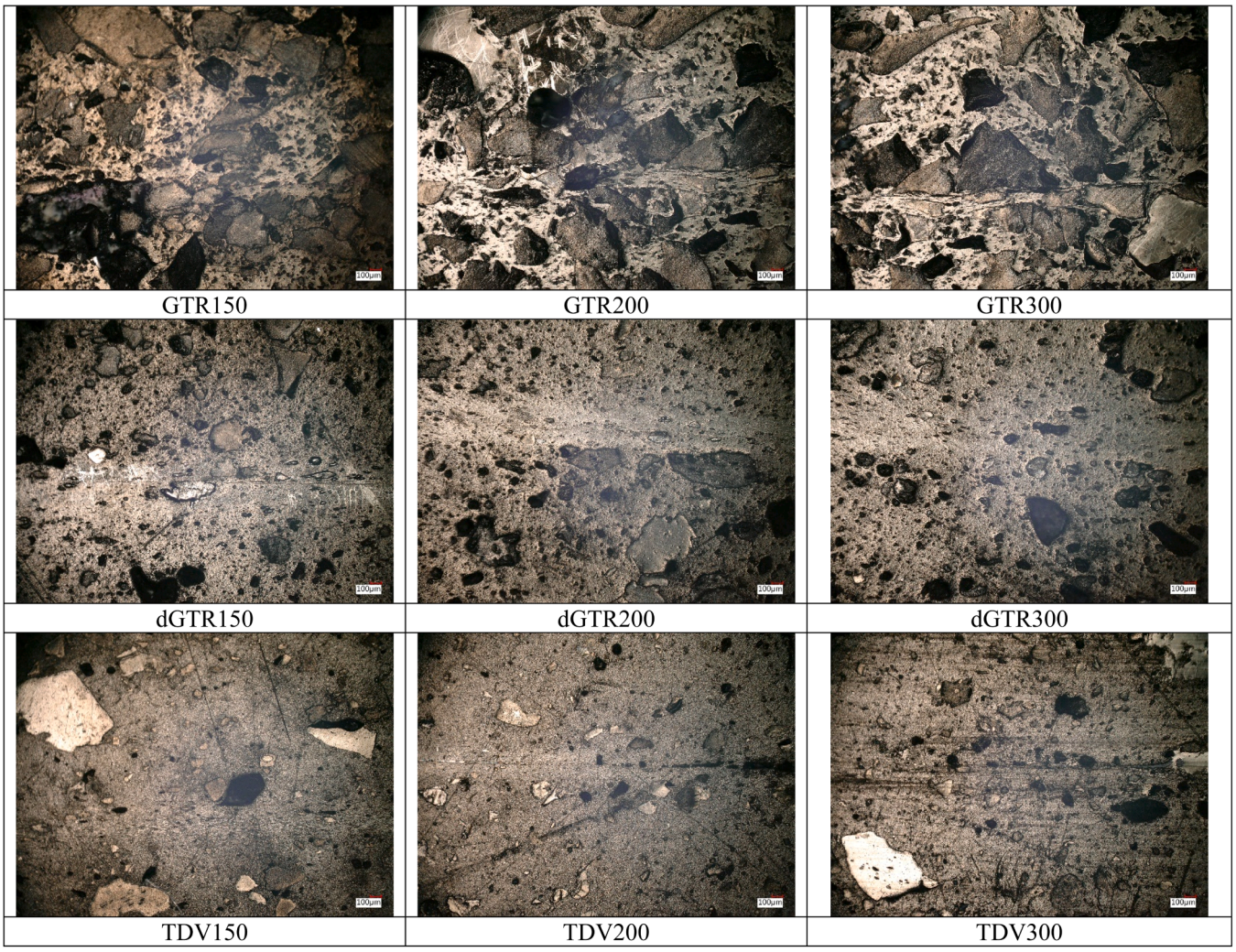

Fig. 7. Morphology of the welds between the blends.

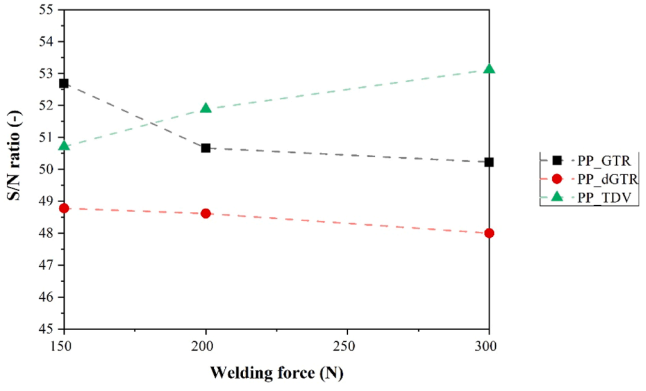

Fig. 8. Interaction plot for the welds between the blends and PP.

process, the weaker damping capacity of the PP phase (Fig. 1) enables vibrations to propagate to the rubber domains, leading to their degradation. Ultrasonic loads induce the breaking of sulfur-sulfur and carbon-sulfur bonds even under a second, this is exploited during ultrasonic devulcanization [39]. In our case, some degree of devulcanization can take place at the outer surface of the GTR. If the weld force is right, this can increase the connection between welded specimens, but if the force is too big, it will cause degradation.

Table 10
S/N ratios for the welds between the blends and PP.

	Welding force (N)	Maximum force (MPa)	S/N (-)
PP_GTR150	150	431,3	52,69
PP_GTR200	200	341,4	50,66
PP_GTR300	300	324,5	50,22
PP_dGTR150	150	274,6	48,77
PP_dGTR200	200	269,6	48,61
PP_dGTR300	300	251,1	47,99
PP_TDV150	150	343,1	50,70
PP_TDV200	200	392,9	51,88
PP_TDV300	300	452,7	53,11

In the case of the welding of PP with PP_dGTR, increasing welding force reduces both maximum tensile force and elongation. This can be caused by the already degraded rubber backbone in the dGTR, as our previous results show [40]. The molecular chains degraded even more due to compounding and the concentrated stress caused by welding.

As for the welding of PP with PP_TDV, a different kind of trend can be observed: increasing the weld force increases both maximum force and elongation and decreases the deviation. This can be connected to a more uniform dispersion of the rubber particles (due to the dynamic vulcanization process). Smaller rubber domains are also more prone to the devulcanization effect, which means this is more significant than the GTR-filled welds.

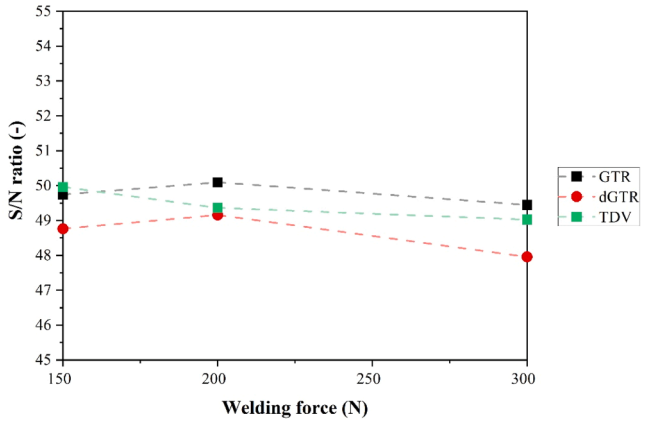

Fig. 9. Interaction plot of the welds between the blends.

Table 11
S/N ratios of the welds between the blends.

	Welding force (N)	Maximum force (MPa)	S/N (-)
GTR150	150	307.1	49.75
GTR200	200	319.7	50.09
GTR300	300	296.6	49.44
dGTR150	150	274.2	48.76
dGTR200	200	286.9	49.15
dGTR300	300	249.8	47.95
TDV150	150	314.7	49.96
TDV200	200	293.8	49.36
TDV300	300	282.6	49.02

As for the weld efficiency, all of the materials behaved similarly. Increased weld forces result in a concentrated energy, which causes the welding to be shorter. The most pronounced decrease can be observed in the case of the welding of PP/PP_TDV, which can be associated with the most uniform dispersion of the rubber domains.

3.4. Microscopy

We examined the morphology of the seams (Fig. 5). A clear seam can be seen on each picture without any bubbles or voids in the welds. This suggests a good connection between the joint surfaces granted by the polypropylene phase of the blends. It can also be observed that the size of the rubber domains decreases in size as an effect of devulcanization and dynamic vulcanization, and their distribution improves. We also detected a core-shell type of morphology: the larger rubber particles tend to stay in the core of the material, whereas the smaller particles are located in the shell part of the specimens. This can help to create a good weld, as the bigger rubber crumbs would hinder the connection between the thermoplastic phases of the specimens.

We also observed that increasing the weld force makes the surface flatter, while at lower forces, we experienced some surface roughness. This is most evident in the case of the PP_TDV weld, the PP phase was able to cross into the TDV phase. This can also explain why the PP_GTR and PP_dGTR specimens broke in the weld, but not the PP_TDV150: this "bridge" of PP was able to behave as a form-locking mechanism that holds the weld together. This effect can be caused by a lower weld force that permits the material to form better than higher weld forces.

3.5. Welding of the blends

We performed the welding tests of the blends (Fig. 6, Table 9). These welds exhibit lower maximum force and higher extensions compared to the welds in the previous round. This is because the increased rubber content of the welded materials toughens the weld.

As for the effect of weld forces, a similar trend can be seen in the case of GTR and dGTR-filling: with increasing weld force, the maximum force and extension tend to decrease due to the devulcanization effect. In the case of the TDV-welds, increasing welding force decreases maximum force but increases the elongation. This can be attributed to the improvement in the connection of the specimens, nearing the properties of a TDV. This improvement can be associated with the good dispersion of rubber particles, which were activated due to the ultrasonic loads.

The weld efficiency also shows a similar trend compared to the last round: increasing weld force results in a decrease in weld efficiency due to the more concentrated force dispersion. We also noted that the values are generally higher compared to the welds with polypropylene. The joining of the same materials can cause, as the similar molecular structure tends to form a better connection.

3.6. Microscopy of the welded blends

We observed the morphology of the seam of the welded blends (Fig. 7), and we saw that the weld lines generally become more visible with increasing the weld force. This can be caused by increasing pressure, which does not allow the formulation of the rough interface between the sheets.

We can also observe the orientation of the rubber particles in the vicinity of the weld. Generally, the welding force and the ultrasonic loads can change the orientation because of the material flow. Before welding, they are disoriented; their position is randomized. As a result of the welding, they tend to have a horizontal orientation parallel to the weld line. This could lead to an improved connection, as the rubber particles are pushed out of the weld, and they do not form vacancies at the weld line.

3.7. Taguchi analysis

The Taguchi analysis of the welds between the blends and polypropylene (Fig. 8, Table 10) reveals that the weld with the best load bearing capacity was the PP_TDV_300N. It can also be seen that the S/N ratio for the PP_GTR welds detiorated with increasing welding force, the PP-dGTR welds were mostly unaffected, and the PP_TDV welds improved with increasing welding force.

The analysis of the welds between the blends (Fig. 9, Table 11) reveals that the best weld is achieved between the GTR-filled PPs with 200 N. However, it is important to note that the difference between values is much smaller compared to the ones in the case of welds between PP and blends.

4. Conclusions

We prepared specimens with ultrasonic welding using polypropylene and polypropylene-ground tire rubber blends utilizing both devulcanization and dynamic vulcanization. We found that the damping of the blends resembled that of the PP rather than rubbers. This made them suitable for ultrasonic welding.

We examined the effect of welding times and found that the most ideal would be 0.3 s, as less time would not allow for mobility, and more time would degrade the molecular structure. We examined the effect of welding force and found a devulcanization effect during welding: the molecules of the GTR-filling were activated when selecting the right parameters, resulting in a better weld. This was most advantageous in the case of TDVs, as the rubber filling was distributed better than in any other blends.

In the case of the welds of the blends, we found similar trends compared to the welds of PP and blends. The difference was due to the increased amount of rubber filling in the weld compared to the PP/blend welds. We also found a devulcanization effect in this round of examinations.

We examined the morphology of the welds on cross-sections and

found that increasing weld force results in a more concentrated and flat weld geometry. We also found that the increasing weld force orients the rubber particles parallel to the weld line. We believe this work is an important step in inserting ground tire rubber into the circular economy by providing an interesting application: joining cheap rubber-like parts with the help of ultrasonic welding can have multiple practical applications in the automotive industry.

CRediT authorship contribution statement

Ákos Görbe: Writing – original draft, Methodology, Investigation, Formal analysis, Data curation, Conceptualization. **Péter Széplaki:** Validation, Methodology, Investigation, Formal analysis, Data curation. **Tamás Bárány:** Writing – review & editing, Supervision, Resources, Project administration, Conceptualization.

Declaration of competing interest

The authors declare the following financial interests/personal relationships which may be considered as potential competing interests:

Tamas Barany reports financial support was provided by National Research Development and Innovation Office. If there are other authors, they declare that they have no known competing financial interests or personal relationships that could have appeared to influence the work reported in this paper.

Acknowledgement

Project no KDP-IKT-2023-900-I1-00000957/0000003 has been implemented with the support provided by the Ministry of Culture and Innovation of Hungary from the National Research, Development and Innovation Fund, financed under the KDP-2023 funding scheme. This work was supported by the National Research, Development and Innovation Office, Hungary (K146085 and 2021-1.1.4-GYORSÍTÓSÁV-2022-00030). Project no TKP-6-6/PALY-2021 has been implemented with the support provided by the Ministry of Culture and Innovation of Hungary from the National Research, Development and Innovation Fund, financed under the TKP2021-NVA funding scheme.

Data availability

Data will be made available on request.

References

[1] D. Gere, T. Czigany, Future trends of plastic bottle recycling: compatibilization of PET and PLA, Polym. Test. 81 (2020) 106160, https://doi.org/10.1016/j.polymertesting.2019.106160.
[2] M.S. Abbas-Abadi, M. Kusenberg, H.M. Shirazi, B. Goshayeshi, K.M. Van Geem, Towards full recyclability of end-of-life tires: challenges and opportunities, J. Clean. Prod. 374 (2022) 29, https://doi.org/10.1016/j.jclepro.2022.134036.
[3] A. Pegoretti, Material circularity in rubber products, Express. Polym. Lett. 17 (2023) 352, https://doi.org/10.3144/expresspolymlett.2023.25. -352.
[4] J. Malaiškienė, T. Astrauskas, T. Januševičius, O. Kizinievič, V. Kizinievič, Potential applications of rubber buffing dust and recovered crumb rubber in cement concrete, Results. Eng. 24 (2024) 103266, https://doi.org/10.1016/j.rineng.2024.103266.
[5] A. Fazli, D. Rodrigue, Recycling waste tires into ground tire rubber (GTR)/rubber compounds: a review, J. Compos. Sci. 4 (2020) 103, https://doi.org/10.3390/jcs4030103.
[6] H. Chittella, L.W. Yoon, S. Ramarad, Z.-W. Lai, Rubber waste management: a review on methods, mechanism, and prospects, Polym. Degrad. Stab. 194 (2021) 109761, https://doi.org/10.1016/j.polymdegradstab.2021.109761.
[7] J. Karger-Kocsis, L. Mészáros, T. Bárány, Ground tyre rubber (GTR) in thermoplastics, thermosets, and rubbers, J. Mater. Sci. 48 (2013) 1–38, https://doi.org/10.1007/s10853-012-6564-2.
[8] M.D. Nazzal, M.T. Iqbal, S.S. Kim, A.R. Abbas, M. Akentuna, T. Quasem, Evaluation of the long-term performance and life cycle costs of GTR asphalt pavements, Constr. Build. Mater. 114 (2016) 261–268, https://doi.org/10.1016/j.conbuildmat.2016.02.096.
[9] S. Ramarad, M. Khalid, C.T. Ratnam, A.L. Chuah, W. Rashmi, Waste tire rubber in polymer blends: a review on the evolution, properties and future, Prog. Mater. Sci. 72 (2015) 100–140, https://doi.org/10.1016/j.pmatsci.2015.02.004.
[10] K. Formela, J. Korol, M.R. Saeb, Interfacially modified LDPE/GTR composites with non-polar elastomers: from microstructure to macro-behavior, Polym. Test. 42 (2015) 89–98, https://doi.org/10.1016/j.polymertesting.2015.01.003.
[11] A. Fazli, D. Rodrigue, Waste rubber recycling: a review on the evolution and properties of thermoplastic elastomers, Materials. (Basel) (2020) 13, https://doi.org/10.3390/ma13030782.
[12] A. Belhaoues, S. Benmesli, F. Riahi, Compatibilization of natural rubber–polypropylene thermoplastic elastomer blend, J. Elastom. Plastics 52 (2020) 728–746, https://doi.org/10.1177/0095244319891231.
[13] P. Wisniewska, S.F. Wang, K. Formela, Waste tire rubber devulcanization technologies: state-of-the-art, limitations and future perspectives, Waste Manage. 150 (2022) 174–184, https://doi.org/10.1016/j.wasman.2022.07.002.
[14] L. Bockstal, T. Berchem, Q. Schmetz, A. Richel, Devulcanisation and reclaiming of tires and rubber by physical and chemical processes: a review, J. Clean. Prod. 236 (2019) 117574, https://doi.org/10.1016/j.jclepro.2019.07.049.
[15] D.Á. Simon, T. Bárány, Effective thermomechanical devulcanization of ground tire rubber with a co-rotating twin-screw extruder, Polym. Degrad. Stab. 190 (2021) 109626, https://doi.org/10.1016/j.polymdegradstab.2021.109626.
[16] S. Seghar, L. Asaro, M. Rolland-Monnet, N.A. Hocine, Thermo-mechanical devulcanization and recycling of rubber industry waste, Resour. Conserv. Recycl. 144 (2019) 180–186, https://doi.org/10.1016/j.resconrec.2019.01.047.
[17] H. Yazdani, M. Karrabi, I. Ghasmi, H. Azizi, G.R. Bakhshandeh, Devulcanization of waste tires using a twin-screw extruder: the effects of processing conditions, J. Vinyl Additive Technol. 17 (2011) 64–69, https://doi.org/10.1002/vnl.20257.
[18] A. Rodak, J. Haponiuk, S. Wang, K. Formela, Investigating the combined effects of devulcanization level and carbon black grade on the SBR/GTR composites, Express. Polym. Lett. 18 (2024) 1191–1208, https://doi.org/10.3144/expresspolymlett.2024.91.
[19] J.I. Gumede, B.G. Hlangothi, C.D. Woolard, S.P. Hlangothi, Organic chemical devulcanization of rubber vulcanizates in supercritical carbon dioxide and associated less eco-unfriendly approaches: a review, Waste Manage. Res. 40 (2022) 490–503, https://doi.org/10.1177/0734242x211008515.
[20] D.Á. Simon, T. Bárány, Microwave devulcanization of ground tire rubber and its improved utilization in natural rubber compounds, ACS Sustain. Chem. Eng. 11 (2023) 1797–1808, https://doi.org/10.1021/acssuschemeng.2c05984.
[21] D.Á. Simon, D.Z. Pirityi, T. Bárány, Devulcanization of ground tire rubber: microwave and thermomechanical approaches, Sci. Rep. 10 (2020) 16587, https://doi.org/10.1038/s41598-020-73543-w.
[22] O. Buitrago-Suescún, R. Britto, Devulcanization of ground tire rubber: thermo-oxidation followed by microwave exposure in the presence of devulcanizing agent, Iran. Polym. J. 29 (2020) 553–567, https://doi.org/10.1007/s13726-020-00818-4.
[23] A.S. Mohite, Y.D. Rajpurkar, A.P. More, Bridging the gap between rubbers and plastics: a review on thermoplastic polyolefin elastomers, Polym. Bullet. 79 (2021) 1309–1343, https://doi.org/10.1007/s00289-020-03522-8.
[24] J.G. Drobny, Handbook of Thermoplastic Elastomers,2nd Edition, 2nd Edition, Elsevier Inc., Oxford, 2014.
[25] A. Kohári, T. Bárány, Sustainable thermoplastic elastomers based on thermoplastic polyurethane and ground tire rubber, J. Appl. Polym. Sci. 141 (2024) e56157, https://doi.org/10.1002/app.56157.
[26] N. Ning, S. Li, H. Wu, H. Tian, P. Yao, G.-H. Hu, M. Tian, L. Zhang, Preparation, microstructure, and microstructure-properties relationship of thermoplastic vulcanizates (TPVs): a review, Prog. Polym. Sci. 79 (2018) 61–97, https://doi.org/10.1016/j.progpolymsci.2017.11.003.
[27] N. Ghahramani, K.A. Iyer, A.K. Doufas, S.G. Hatzikiriakos, Rheology of thermoplastic vulcanizates (TPVs), J. Rheol. (N. Y. N. Y) 64 (2020) 1325–1341.
[28] A. Kohári, T. Bárány, Development of thermoplastic vulcanizates based on in situ synthesized thermoplastic polyurethane and acrylonitrile-butadiene rubber: the influence of the curing system, J. Polym. Res. 29 (2022) 361, https://doi.org/10.1007/s10965-022-03176-2.
[29] C. Nakason, C. Manleh, N. Lopattananon, A. Kaesaman, The influence of crosslink characteristics on key properties of dynamically cured NR/PP blends, Express. Polym. Lett. 18 (2024) 487–503, https://doi.org/10.3144/expresspolymlett.2024.36.
[30] A. Kohári, I.Z. Halász, T. Bárány, Thermoplastic Dynamic Vulcanizates with In Situ Synthesized Segmented Polyurethane Matrix, Polymers. (Basel) 11 (2019) 1663.
[31] G. Holden, Thermoplastic elastomers. *Abstracts of Papers of the*, 219, American Chemical Society, 2000, p. U549. -U549.
[32] A. Thitithammawong, C. Hayichelaeh, W. Nakason, N. Jehvoh, The use of reclaimed rubber from waste tires for production of dynamically cured natural rubber/reclaimed rubber/polypropylene blends: effect of reclaimed rubber loading, J. Metals, Mater. Minerals (2019) 29.
[33] F.A. Mohd Khairuddin, A.A. Rashid, C.P. Leo, G.K. Lim, A.L. Ahmad, H.M. Lim, I.C. S. Tan, Recent progress in superhydrophobic rubber coatings, Prog. Org. Coat. 171 (2022) 107024, https://doi.org/10.1016/j.porgcoat.2022.107024.
[34] Rotheiser, J. Joining of Plastics. In *Joining of Plastics*; pp. i–xxxii.
[35] A. Benatar, 12 - Ultrasonic welding of plastics and polymeric composites, in: J. A. Gallego-Juárez, K.F. Graff (Eds.), Power Ultrasonics, Woodhead Publishing, Oxford, 2015, pp. 295–312.
[36] S.K. Bhudolia, G. Gohel, K.F. Leong, A. Islam, Advances in Ultrasonic Welding of Thermoplastic Composites: a Review, Materials. (Basel) 13 (2020) 1284.
[37] H. Li, C. Chen, R. Yi, Y. Li, J. Wu, Ultrasonic welding of fiber-reinforced thermoplastic composites: a review, Int. J. Adv. Manuf. Technol. 120 (2022) 29–57, https://doi.org/10.1007/s00170-022-08753-9.

[38] S. Jalali, M. Baniadam, M. Maghrebi, Impedance value prediction of carbon nanotube/polystyrene nanocomposites using tree-based machine learning models and the Taguchi technique, Results. Eng. 24 (2024) 103599, https://doi.org/10.1016/j.rineng.2024.103599.

[39] A. Isayev, J. Chen, A. Tukachinsky, Novel ultrasonic technology for devulcanization of waste rubbers, Rubber Chem. Technol. 68 (1995) 267–280.

[40] Á. Görbe, A. Kohári, T. Bárány, Rubber compounds from devulcanized ground tire rubber: recipe formulation and characterization, Polymers 16 (2024) 455.